The Impact of Carbon Concentration on the Crystalline Phase and Dielectric Constant of Atomic Layer Deposited HfO_2 Films on Ge Substrate

Hyung-Suk Jung, Sang Ho Jeon, Hyo Kyeom Kim, Il-Hyuk Yu, Sang Young Lee, Joohwi Lee, Yoon Jang Chung, Deok-Yong Cho, Nae-In Lee, Tae Joo Park, Jung-Hae Choi, Seungwu Han and Cheol Seong Hwang

ECS J. Solid State Sci. Technol. 2012, Volume 1, Issue 2, Pages N33-N37.
doi: 10.1149/2.020202jss

ECS Journal of Solid State Science and Technology, **1** (2) N33-N37 (2012)
2162-8769/2012/1(2)/N33/5/$28.00 © The Electrochemical Society

The Impact of Carbon Concentration on the Crystalline Phase and Dielectric Constant of Atomic Layer Deposited HfO_2 Films on Ge Substrate

Hyung-Suk Jung,[a] Sang Ho Jeon,[a] Hyo Kyeom Kim,[a] Il-Hyuk Yu,[a] Sang Young Lee,[a] Joohwi Lee,[a] Yoon Jang Chung,[a] Deok-Yong Cho,[a] Nae-In Lee,[b] Tae Joo Park,[c] Jung-Hae Choi,[d] Seungwu Han,[a] and Cheol Seong Hwang[a,z]

[a]*WCU Hybrid Materials Program, Department of Materials Science and Engineering and Inter-University Semiconductor Research Center, Seoul National University, Seoul 151-744, Korea*
[b]*TD3 Team, System LSI Division, Samsung Electronics Co. Ltd, Gyeonggido 446-712, Korea*
[c]*Department of Materials Engineering, Hanyang University, Ansan 426-791, Korea*
[d]*Electronic Materials Research Center, Korea Institute of Science and Technology, Seoul 136-791, Korea*

The effect of the carbon concentration on the crystalline phase and dielectric constant (k) of atomic layer deposited HfO_2 films on Ge substrate was investigated. After annealing, the HfO_2 films grown at 200°C and 280°C were crystallized to the tetragonal (*t*) and monoclinic (*m*) phases, respectively, which was related to the carbon contents within the films and grain boundary energy. To clarify this, the energy difference between a *t*- and a *m*- phases (ΔE_{tetra}) was calculated by first principles calculations. The higher k value of *t*-HfO_2 compared to amorphous and monoclinic HfO_2 was experimentally confirmed.
 [DOI: 10.1149/2.020202jss]

Manuscript submitted April 17, 2012; revised manuscript received May 29, 2012. Published July 20, 2012.

Increasing dielectric constant (k) of high-k dielectrics, such as HfO_2, is still an important research topic for next generation complementary metal oxide semiconductor (CMOS) devices because an equivalent oxide thickness (EOT) far lower than 1 nm will be necessary soon.[1] The k values of several high-k dielectrics are usually dependent on their crystalline structure, and HfO_2 also shows the same behavior. At atmospheric pressure, HfO_2 has three polymorphs of cubic (*c*), tetragonal (*t*) and monoclinic (*m*) phases. The k value of the monoclinic phase is similar to the amorphous phase (∼15), while those of the cubic and tetragonal phases are significantly higher compared to these two phases.[2,3] However, the monoclinic phase is the most stable phase at room temperature, and HfO_2 films are usually crystallized into this state. As the tetragonal phase of HfO_2 requires temperatures higher than ∼2000 K, attempts to achieve this phase at room temperature through the introduction of dopants into the HfO_2 films have been widely studied, both experimentally and theoretically.[4–7] Several papers reported that carbon contents in the HfO_2 films on Si substrate increased with decreasing deposition temperature, causing the stabilization of the tetragonal (or cubic) phase.[8,9] However, atomistic mechanism for such stabilization is still under debate. Fischer et al. reported that the tendency to stabilize the tetragonal phase is strongly dependent on the kind of dopant used, including Si, C, Ge, Ti, Se, and Ce, and that their ionic size plays a crucial role in the stabilization mechanism.[7] The study also reported that the carbon atoms substituting Hf in HfO_2 cannot stabilize the tetragonal phase. However, other possible impurity incorporation mechanisms were not considered. Therefore, one cannot exclude the possibility that the carbon can stabilize the tetragonal phase.

When the dopant or impurity density is rather high, they can actually interact with each other or even can induce the formation of different type of defects, such as oxygen vacancy, which have been rarely considered in the theoretical works at earlier time. This was partly due to the limited computing power since considering these types of interactions requires a much larger model size, which makes the computation very expensive. However, it is clear that the defect association is indispensable for the accurate understanding of the phase transition induced by the doping (or remaining impurity) as will be shown in this work.

Another notable finding from several theoretical works is that the absolute molar free energy of the tetragonal or cubic phase is still higher than that of monoclinic phase even though the difference decreases with the doping concentration. This is in contradiction with many experimental observations where the transition of the phase from the monoclinic into the other crystalline phases is indeed observed. One critical difference between the theoretical and experimental works lies on the ignorance (theoretical works) and existence (experimental works) of interface or grain boundaries. In fact, another high-k film, ZrO_2, which has the same crystal structures as HfO_2, showed the transition of its crystal structure from the stable monoclinic to tetragonal (or cubic) one even without any intentional doping or high temperature annealing.[10–14] Such a transition has been more often observed from the metal/insulator/metal structure (MIM), where metal is usually TiN, comparing with the metal/insulator/semiconductor structure (MIS).[12] This has been extensively used in capacitor of dynamic random access memory to achieve a higher capacitance. In fact, such a transition into the meta-stable or unstable phases of ZrO_2 has been well understood in the bulk-ceramics researches.[13,14] In those works, the ceramic materials with smaller grain size evidently tend to show the meta-stable or unstable phases which was attributed to the higher surface or grain boundary energy of the lower symmetry phase (monoclinic) compared with that of the higher symmetry phase (tetragonal and cubic). When the grain size becomes small enough for the lowering of grain boundary energy by the phase transition to overcome the bulk-energy cost for the phase transition, the poly-crystalline aggregate material becomes to have the structure of higher-k value. The same mechanism may well be applied to the poly-crystalline ZrO_2 thin films, of which grain size is usually much smaller compared with the bulk ceramic materials.

However, such a transition from the monoclinic to tetragonal (cubic) phase by the grain size effect has rarely been observed in HfO_2 films unless other driving forces such as doping (impurity, vacancy) or local epitaxial constraint exist.[15] This might be due to the smaller surface or grain boundary energy difference across the phases or stronger bulk energy effect, i. e. the bulk energy difference between the meta (unstable)-stable phases and stable phase is large enough to negate the surface or grain boundary effect. In fact, it has been reported that the average grain size of HfO_2 film is usually larger than that of ZrO_2 film even when they were prepared under identical atomic layer deposition (ALD) conditions except for the metal precursors (but still the ligands of the Hf- and Zr-precursors are the same).[11] Therefore, It could well be that some level of doping or some other method is required in HfO_2 to achieve the desired phase transition.

Unequivocal identification of the origins for such a transition in MIS system appears to be more complicated compared with the MIM case due to the involvement of several other uncontrollable factors, including intermixing of the high-k film and substrate material during the film growth or post-deposition annealing (PDA). Especially, when

[z]E-mail: cheolsh@snu.ac.kr

the high-k films are deposited on Ge substrate, which is generally more reactive than Si mainly due to the lack of stable interfacial oxide layer (GeO_2), this problem becomes even more serious. Ge channel devices have drawn a great deal of attention as next generation CMOS devices due to its higher electron (x2) and hole (x4) mobility compared to Si. The phase transition of ZrO_2 film into the higher-k phase grown on Ge substrate has been observed and attributed to the diffusion of Ge into the films.[16] However, there could be other factors leading to the transition, as will be discussed in this work, but systematic investigation on the phase transition of HfO_2 on Ge has rarely been reported despite its technical importance. Several earlier works may not lead to the definite conclusion because of disparate process conditions. Therefore, in this work, the phase evolution behaviors of HfO_2 film on Ge substrate will be carefully examined by comparing them with the corresponding results on Si substrate, which is much better understood, under the well-controlled deposition conditions.

In the present study, the authors focused on the role of remnant carbon (C) atoms in the film since the influence of Ge-diffusion can be obviously excluded as shown later. In ALD, there could be two typical methods to control the remaining C concentration; changing the growth temperature (T_g) and varying the oxygen source concentration. The lower T_g and lower oxygen source concentration generally result in higher impurity concentrations due to the incomplete ALD reaction. The effects of different oxygen source concentration on the phase evolution and other chemical properties of HfO_2 films are reported in detail elsewhere,[17] where the C impurity interrupted the growth of HfO_2 grains and form smaller grains which eventually ended up with the tetragonal (cubic) phase. Even though this was a viable approach to enlighten the origin of phase transition, the role of substrate material (or inter-diffusion) on this phenomenon can hardly be identified because the oxygen source concentration hardly influenced the inter-diffusion. Therefore, changing the T_g is a viable approach since it can influence the diffusion of substrate material into the film as well as changing the impurity concentration. In fact, this method bears another merit especially on Ge substrate; the implementation of ALD HfO_2 on Ge substrates has been hindered by the reaction between the film and substrate during the deposition process, which results in the degradation of its structural and electrical properties.[18,19] A typical example of this is the presence of large hysteresis in the capacitance-voltage (C-V) measurement. Such hysteresis originates from the intermixing between HfO_2 and the (oxidized) Ge atoms, and creates electrically active defects near the interface or in the bulk dielectric film.[8,19] Therefore, it is necessary to minimize the reaction between HfO_2 and Ge substrates for this technology to be available. The authors reported elsewhere that the C-V hysteresis and charge trapping properties of HfO_2 films on Ge substrates were largely improved when decreasing the deposition temperature from 280°C to 200°C, although an opposite trend is observed on Si substrates.[8]

In this study, therefore, the effect of carbon concentration on the crystalline phase and dielectric constant of HfO_2 films deposited at low temperatures was examined by experimental and theoretical studies. In particular, various possible sites that the carbon atoms may occupy were considered in first-principles calculations to clarify whether the incorporated carbon can stabilize the tetragonal phase of the HfO_2 matrix. The influence of Ge incorporation on the stabilization of the tetragonal phase was also considered, but it was excluded from the present report due to reasons explained in the experimental results section below.

Experimental

Metal Oxide Semiconductor (MOS) capacitor devices were fabricated on p-type Ge substrates (resistivity ~0.02 Ωcm, size ~2 × 2 cm), which were cleaned through cyclic cleaning process involving a diluted HF (1%) dip and a deionized water rinse. After wet cleaning, HfO_2 films were deposited in a 4-in.-diameter cold (~100°C) wall, traveling wave type ALD reactor at various wafer temperatures ranging from 160°C to 280°C. TEMAHf ($Hf[N(C_2H_5)(CH_3)]_4$) and ozone (concentration of 170 g/m^3) were used as the Hf precursor and the oxygen source, respectively. PDA was performed at various temperatures ranging from 400°C to 650°C in a N_2 ambient for 30 seconds. For comparison, the HfO_2 films were also prepared on a Si substrate with identical conditions to the Ge substrate. Sputtered Pt electrode (~80 nm) was deposited as the top electrode through a shadow mask to define the gate electrode. Finally, forming gas annealing was performed in a $N_2 + H_2$ (5%) ambient at 400°C. A Hewlett-Packard (HP) 4155 semiconductor parameter analyzer and a HP 4284 LCR meter were used for the electrical characterization of the MOS capacitor devices.

The chemical bonding states of HfO_2 on Si and Ge substrates were examined by the X-ray photoelectron spectra (XPS) of the C 1s, and Ge $2p_{3/2}$. The XPS measurement was carried out using a Sigma Probe (ThermoVG) system equipped with a monochromatic Al Kα source (1486.6 eV) for the excitation of photoelectrons. The positions of all peaks were calibrated for the C 1s peak of the substrate to be at 284.5 eV. Carbon impurity concentration was confirmed by Auger electron spectroscopy (AES, Perkin-Elmer 660) in depth profiling mode, which is done by the Ar^+ ion sputtering.

The thicknesses of the deposited high-k gate dielectrics were measured by ellipsometry which was calibrated by the more accurate estimation method of X-ray reflectivity (XRR) and transmission electron microscopy (TEM) measurements. The XRR experiments were carried out using a PANalytical X'Pert materials research diffractometer. Moreover, the crystalline structure of the films was examined by glancing angle incidence X-ray diffraction (GAXRD).

In order to investigate the microscopic origin of this phenomenon, first-principles calculations based on the density function theory were carried out on the thermodynamic conditions of carbon incorporated HfO_2 films. The VASP code was used for the computation of total energies and structural optimizations. Supercells constructed from 96 atomic sites were used for all structures. Details on the calculation methods were reported elsewhere.[6]

Results and Discussion

The ALD temperature strongly affects the impurity concentration in HfO_2 films.[20] Figure 1a shows AES depth profiles of carbon in the HfO_2 films deposited at the various temperatures ranging from 160°C to 280°C on Ge substrate. The carbon content within the films increases with decreasing deposition temperature. At low deposition temperatures, TEMAHf precursors are known to have incomplete chemical reactions, which is what causes this type of impurity incorporation.[20] In addition, it was confirmed that carbon concentration in the film was not notably changed after the PDA (data not shown).

The incorporation of Ge by the diffusion from substrate during the ALD and PDA was examined using X-ray photoelectron spectroscopy (XPS). Thin HfO_2 films (~1.5 nm) were deposited at 200°C (200-HfO_2) and 280°C (280-HfO_2) on Ge substrates and annealed at 600°C.

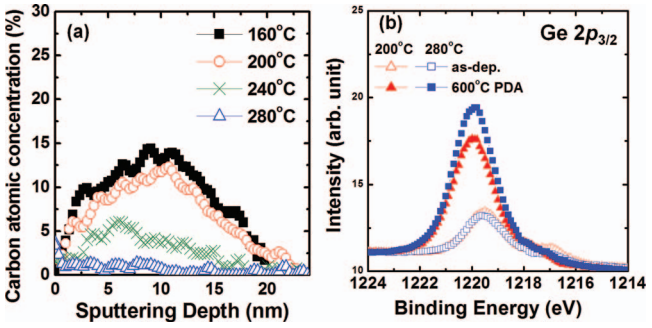

Figure 1. (Color online). (a) AES depth profiles of carbon in the HfO_2 films deposited at various temperatures ranging from 160°C to 280°C. (b) XPS spectra of Ge $2p_{3/2}$ peaks for the HfO_2 films deposited at 200°C and 280°C before and after PDA at 600°C in N_2 ambient.

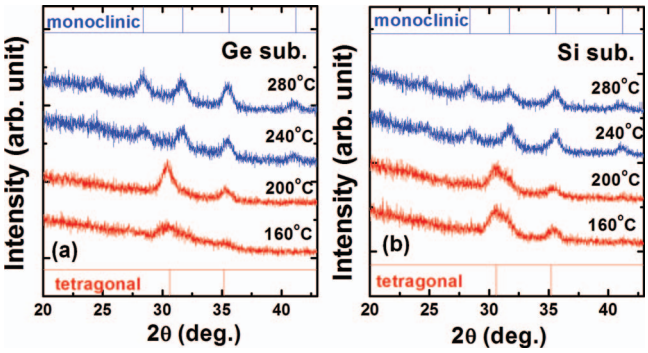

Figure 2. (Color online). GAXRD spectra of the HfO_2 films annealed at 600°C on (a) Ge and (b) Si substrate.

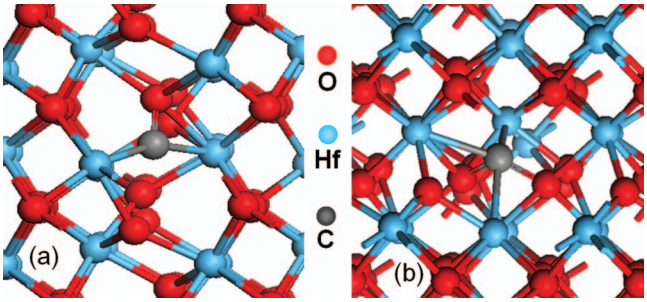

Figure 3. (Color online). Atomic structures around the introduced interstitial carbon in (a) *m*-HfO_2 and (b) *t*-HfO_2.

Figure 1b shows XPS spectra of Ge $2p_{3/2}$ peaks from the 200-HfO_2 and 280-HfO_2 samples before and after PDA. The as-deposited 200-HfO_2 and 280-HfO_2 films show strong oxidation peaks at the binding energy around 1219.6 eV which is ∼2.6 eV higher than that of the Ge substrate peak (∼1217 eV), and negligible difference in the peak shape and position was observed between the two films. Considering that the ALD-HfO_2/Ge interface did not show any notable interfacial oxide layer (GeO_x),[8,21] the significant XPS peak of oxidized Ge could be from the oxidized Ge in the bulk HfO_2 film or on the film surface.[21] After the PDA process, the intensity of Ge oxide peaks significantly increased, suggesting the further diffusion of Ge into the HfO_2 film. Compared to the 200-HfO_2, 280-HfO_2 shows further increase in the intensity of Ge oxide peaks, suggesting that a higher thermal budget enhances the material interaction between HfO_2 and (oxidized) Ge substrate. Interestingly, the stabilization of tetragonal (or cubic) phase in HfO_2 was observed only in 200-HfO_2 as shown below (Fig. 2), which suggests that the Ge-diffusion is not the major reason for the phase transition in this work.

In order to understand the impact of deposition temperature on crystalline phase of the HfO_2 films, glancing angle incidence X-ray diffraction (GAXRD) data was collected. The GAXRD spectra of the 600°C annealed HfO_2 films deposited at various temperatures on Ge substrates are shown in Fig. 2a. The 280-HfO_2 film and the film deposited at 240°C (240-HfO_2) show a strong peak near $2\theta = 28.5°$, indicating that the crystallized HfO_2 films have a monoclinic phase, while the 200-HfO_2 film and the film deposited at 160°C (160-HfO_2) show a relatively stronger peak near $2\theta = 30.5°$, corresponding to the tetragonal phase and/or a cubic phase. An unequivocal identification on whether the peak corresponds to tetragonal or cubic phase is not possible due to broad diffraction peak shape and similar lattice parameters of two phases. Here, the crystalline phase other than monoclinic was termed as *t*-HfO_2 for the sake of simplicity. When the tetragonal phase is achieved, its dielectric constant is much higher compared to that of the monoclinic or amorphous phase,[2,3] which is also confirmed in this work as shown in Fig. 4. However, on the contrary to the previous report[16] Ge-diffusion was not the major cause for such phase transition as it was discussed in Fig. 1b. Further confirmation for this hypothesis can be found from Fig. 2b, where the GAXRD spectra of the same HfO_2 films on Si substrates are shown. No significant difference in the phase evolution was observed between Ge and Si substrates, suggesting, again, that the diffusion of Ge was not the main cause for the tetragonal phase formation. Si-diffusion may influence the phase evolution, but formation of stable monoclinic phase at higher ALD temperature and formation of meta-stable phase at lower ALD temperature rules out such possibility, since Si diffusion is more effective at higher temperatures. Therefore, it is believed that carbon impurity and/or oxygen vacancies within the HfO_2 films play an important role in crystalline structure transformation.[22]

Next, the energy difference per formula unit (f.u.) between a tetragonal phase and a monoclinic phase (ΔE_{tetra}) was estimated using the first principles method. All calculations were performed using the VASP[23] code within the projector-augmented wave (PAW) potential.[24] The generalized gradient approximation (GGA)[25] was implemented to describe the electron-electron interaction. Using 96-atoms supercell for all structures, a $2 \times 2 \times 2$ k-mesh and a plane wave energy cutoff of 500 eV were used. For the charged systems including V_O^{2+}, the first-order monopole correction[26] was applied to remedy the unphysical electrostatic interaction between periodic defects. The energy of *t*-HfO_2 was higher than *m*-HfO_2 when no defect or dopants were included, and the calculated ΔE_{tetra} in this case (perfect ΔE_{tetra}) is 0.171 eV. To clarify whether the incorporated carbon can stabilize the tetragonal phase of the HfO_2 matrix, three possible sites that the carbon atoms could occupy were considered; interstitial carbon (C_i), substitutional carbon at Hf-sites (C_{Hf}), and substitutional carbon at O-sites (C_o). It was reported that Hf is eightfold coordinated and the oxygen atoms are fourfold coordinated in *t*-HfO_2, while Hf is sevenfold coordinated and the oxygen atoms are threefold (O3) and fourfold (O4) coordinated with the nearby Hf atoms in *m*-HfO_2.[27] For interstitial carbon atoms, the minimum energy was found to exist when carbon atoms were placed in the large void of the O3 layer in the *m*-HfO_2 structure and in the Hf layer of the *t*-HfO_2 structure, as shown in Figs. 3a and 3b, respectively. Table I shows the calculated ΔE_{tetra} of the HfO_2 structures when carbon was incorporated by the various doping types. A lower ΔE_{tetra} of 0.164 eV was observed for C_i, suggesting that it tends to stabilize the tetragonal phase. In addition, when carbon substitutes Hf or O sites, the calculated ΔE_{tetra} are 0.234 eV and 0.128 eV, respectively. This indicates that a C_{Hf} has almost no tendency to stabilize the tetragonal phase, while a C_o is prone to stabilize the tetragonal phase, which is in good agreement with previous studies.[7]

However, although it has been reported that C_i can interact with Hf atoms and easily generate oxygen vacancies (V_o),[28] no simulations consider this factor. Therefore, in this study, theses aspects were also considered. After introducing carbon atoms into the HfO_2 structures, the calculated oxygen vacancy formation energy of both *t*-HfO_2 and *m*-HfO_2 decrease irrespective of doping type (data not shown), suggesting that oxygen vacancies can be easily generated when a carbon exist in the HfO_2 structures. Therefore, the carbon-oxygen vacancy complex (C-V_o) was also considered when calculating the ΔE_{tetra} of the HfO_2 structures. It was also reported that the presence of a neutral oxygen vacancy (V_o°) slightly affects the ΔE_{tetra}, while ΔE_{tetra} are

Table I. The energy difference per formula unit between the two phases (ΔE_{tetra}) of the HfO_2 films when carbon was incorporated by the various doping types.

	ΔE_{tetra} (eV/f.u.)		
	C	C-V_o°	C-V_o^{+2}
Perfect		0.171	
C_i	0.164	0.155	0.114
C_{Hf}	0.234	0.229	0.081
C_o	0.128	–	–

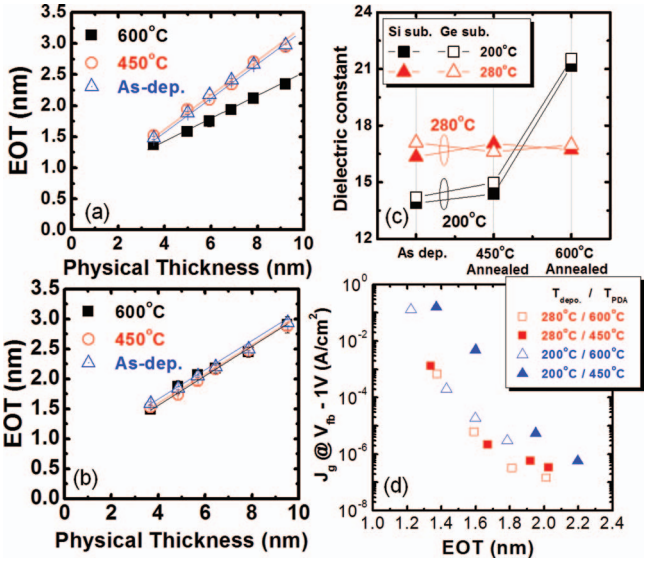

Figure 4. (Color online). EOT vs. T_{phy} plots of (a) 200-HfO_2 and (b) 280-HfO_2 grown on Ge substrates after annealing at various temperatures. (c) The calculated k values of the HfO_2 films grown on Si and Ge substrates prepared at various deposition and PDA temperatures. (d) Variation of dielectric leakage current density (measured at a voltage of V_{FB} – 1V) as a function of EOT of the 200-HfO_2 and 280-HfO_2 samples after the PDA at 450 and 600°C, respectively.

significantly reduced when this vacancy is doubly ionized (V_o^{2+}) in a previous study.[6] Therefore, the energies were calculated for a carbon combined with a V_o° (C-V_o°) and a carbon combined with V_o^{2+} (C-V_o^{2+}), where the carbon atoms were introduced either at the interstitial or Hf substitutional sites. When C_i is introduced and combined with nearby V_o° or V_o^{2+}, the calculated ΔE_{tetra} are 0.155 eV and 0.114 eV, respectively. In addition, when carbon atoms substitute Hf-sites and form C-V_o° and C-V_o^{2+}, the calculated ΔE_{tetra} are 0.229 eV and 0.081 eV, respectively. This suggests that a larger tendency to stabilize the tetragonal phase is observed when carbon atoms that substitute Hf-sites atoms are combined with nearby V_o^{2+}. Even though the above calculations showed that carbon atoms generally have a tendency to stabilize the tetragonal phase, however, the free energy of tetragonal phase is still higher than that of monoclinic phase. Therefore, other reason must be considered which is discussed at the later part of this section.

In order to confirm the effect of crystalline phase on the k, the k values were extracted by plotting the EOT of the as-deposited and PDA films as a function of their physical thickness (T_{phy}). The as-deposited and 450°C annealed HfO_2 films were amorphous, while the 600°C annealed HfO_2 was crystallized, irrespective of deposition temperature.[8] Figures 4a and 4b show the EOT vs. T_{phy} plots of 200-HfO_2 and 280-HfO_2 grown on Ge substrates after annealing at various temperatures. The calculated k values of the HfO_2 films grown on Si and Ge substrates prepared at various deposition and PDA temperatures are summarized in Fig. 4c. The extracted k values of 280-HfO_2 were ~17 regardless of PDA temperature. The insignificant difference between the extracted k values of amorphous and *m*-HfO_2 are in good agreement with previous reports.[2,3] The extracted k value of amorphous 200-HfO_2 was ~14, while that of crystallized 200-HfO_2 was ~21. This increased k value is related to the transformation of microstructure from amorphous to tetragonal (or cubic). The lower k value of the amorphous 200-HfO_2 films compared to the 280-HfO_2 can be explained by the higher concentration of impurities, which induce voids and hydrogen related defects in the films.[20] In addition, compared to the theoretically calculated k value of the carbon incorporated *t*-HfO_2 films (>33),[7] the experimentally extracted k values of *t*-HfO_2 in this work (~21) was lower, suggesting that the films were not fully crystallized with perfect tetragonal phases in this work because crystallization was interrupted by impurities or other defects. Figure 4d shows the variation of dielectric leakage current density (J_g, measured at a voltage of V_{FB} – 1V, where V_{FB} is the flatband voltage estimated from the capacitance – voltage curve) as a function of EOT of the 200-HfO_2 and 280-HfO_2 samples after the PDA at 450 and 600°C, respectively. The as-deposited samples showed a much higher J_g level, so they are not indicated in this graph. Although the films deposited at different T_g have different carbon concentrations at the as-deposited state, they did not show any notable difference in this dielectric performance measure after the PDA at 600°C. This must be due to the fact that the higher k values of the 200-HfO_2 film after the PDA counteract the detrimental influence of the carbon impurity on the J_g. However, after the PDA at 450°C the HfO_2 samples showed certainly degraded performance which may have some relation with the remaining impurity and insufficient defect curing effect. Under this PDA condition, the k value is still remained at the low level so that the beneficial influence of the higher-k value cannot be achieved.

Below, the possible reasons for achieving the higher k values of the 200-HfO_2 samples on both Ge and Si substrates after the PDA at 600°C. As discussed in introduction section, this must have a close correlation with the grain size and accompanying grain boundary energy effect. In ZrO_2, which is of iso-structure with HfO_2, fine grained poly-crystalline films generally show tetragonal phase even without any intentional doping due to the lower grain boundary (or surface) energy of the tetragonal phase compared to that of monoclinic phase.[10–14] It is believed that the same mechanism drives the phase transition here. The average grain size measured by atomic force microscopy (AFM) of the crystallized 200-HfO_2 and 280-HfO_2 are $\sim 36 \pm 10$ and $\sim 58 \pm 22$ nm, respectively (data not shown). Therefore, the 200-HfO_2 sample must be influenced by the grain boundary energy effect more dominantly compared with the other case when they were crystallized after the PDA at 600°C. The incorporation of high content of carbon impurity in the 200-HfO_2 sample interferes with the atomic aggregation of Hf and O atoms, which were mostly remained in amorphous state, during the PDA resulting in the smaller grain size. In addition, the phase transition to the higher-k phase was further strengthened by the lowered ΔE_{tetra} due to the carbon (and V_o association) as shown by the first principles calculation above. The decreased volume free energy difference by carbon effect made the grain boundary effect dominant in determining the crystal structure. It is also noted that the experimental carbon concentration was much higher (10–15%) compared to the calculation model (~1%) so that the actual lowering of ΔE_{tetra} could be even larger.

Conclusion

In summary, the ALD HfO_2 films grown at 200°C had an abnormal tetragonal phase after the PDA, which had a higher dielectric constant than the amorphous and monoclinic phase. The origin of this phenomenon is ascribed to the carbon incorporation into the film. First-principles studies showed that the carbon impurity, either at the interstitial site or at Hf-substitutional site combined with oxygen vacancy, decreases the energy cost of the tetragonal phase over the monoclinic phase which facilitates the phase transition to the higher-k phase. The most direct cause for the phase transition must be the grain boundary energy effect of the polycrystalline HfO_2 films with smaller grain size. The higher k values of the film grown at lower temperature after the PDA at 600°C nullify the undesirable influence of the impurity on the leakage current. Therefore, the J_g – EOT performances of the films grown at 200 and 280°C, respectively, showed almost identical trend after the PDA at 600°C.

Acknowledgments

Authors acknowledge support by Convergent Research Center program (Grant No. 2011K000610) through the National Research Foundation of Korea funded by the Ministry of Education, Science, and Technology, and World Class University program through the

Korea Science and Engineering Foundation funded by the Ministry of Education, Science, and Technology (R31-2008-000-10075-0).

References

1. International Technology Roadmap for Semiconductors (2011).
2. X. Zhao and D. Vanderbilt, *Phys. Rev. B*, **65**, 233106 (2002).
3. T.-J. Chen and C.-L. Kuo, *J. Appl. Phys.*, **110**, 064105 (2011).
4. R. I. Hegde, D. H. Triyoso, S. B. Samavedam, and B. E. White, *J. Appl. Phys.*, **101**, 074113 (2007).
5. K. Tomida, K. Kita, and A. Toriumi, *Appl. Phys. Lett.*, **89**, 142902 (2006).
6. C.-K. Lee, E. Cho, H.-S. Lee, C. S. Hwang, and S. Han, *Phys. Rev. B*, **78**, 012102 (2008).
7. D. Fischer and A. Kersch, *Appl. Phys. Lett.*, **92**, 012908 (2008).
8. H.-S. Jung, H. K. Kim, I.-H. Yu, S. Y. Lee, J. Lee, J. Park, J. H. Jang, S.-H. Jeon, Y. J. Chung, N.-I. Lee, T. J. Park, J.-H. Choi, and C. S. Hwang, *J. Electrochem. Soc.*, **159**, G33 (2012).
9. J. Schaeffer, N. V. Edwards, R. Liu, D. Roan, B. Hradsky, R. Gregory, J. Kulik, E. Duda, L. Contreras, J. Christiansen, S. Zollner, P. Tobin, B.-Y. Nguyen, R. Nieh, M. Ramon, R. Rao, R. Hegde, R. Rai, J. Baker, and S. Voight, *J. Electrochem. Soc.*, **150**, F67 (2003).
10. G. Teufer, *Acta Cryst.*, **15**, 1187 (1962).
11. H.-S. Jung, S.-A. Lee, S.-h. Rha, S. Y. Lee, H. K. Kim, D. H. Kim, K. H. Oh, J.-M. Park, W.-H. Kim, M.-W. Song, N.-I. Lee, and C. S. Hwang, *IEEE Trans. Electron Devices*, **58**, 2094 (2011).
12. S. K. Kim and C. S. Hwang, *Electrochem. Solid-State Lett.*, **11**, G9 (2008).
13. R. C. Garvie, *J. Phys. Chem.*, **69**, 1238 (1965).
14. P. F. Becher and M. V. Swain, *J. Am. Ceram. Soc.*, **75**, 493 (1992).
15. M. Seo, S. K. Kim, J. H. Han, and C. S. Hwang, *Chem. Mater.*, **22**, 4419 (2010).
16. P. Tsipas, S. N. Volkos, A. Sotiropoulos, S. F. Galata, G. Mavrou, D. Tsoutsou, Y. Panayiotatos, A. Dimoulas, C. Marchiori, and J. Fompeyrine, *Appl. Phys. Lett.*, **93**, 082904 (2008).
17. D.-Y. Cho, H.-S. Jung, I.-H. Yu, J. H. Yoon, H. K. Kim, S. Y. Lee, S. H. Jeon, S. Han, J. H. Jeong, T. J. Park, B.-G. Park, and C. S. Hwang, accepted to *Chem. Mater.* (2012).
18. A. Delabie, F. Bellenger, M. Houssa, T. Conard, S. Van Elshocht, M. Caymax, M. Heyns, and M. Meuris, *Appl. Phys. Lett.*, **91**, 082904 (2007).
19. F. Bellenger, M. Houssa, A. Delabie, V. Afanasiev, T. Conard, M. Caymax, M. Meuris, K. De Meyer, and M. M. Heyns, *J. Electrochem. Soc.*, **155**, G33 (2008).
20. X. Liu, S. Ramanathan, A. Longdergan, A. Srivastava, E. Lee, T. E. Seidel, J. T. Barton, D. Pang, and R. G. Gordon, *J. Electrochem. Soc.*, **152**, G213 (2005).
21. D.-Y. Cho, H.-S. Jung, I.-H. Yu, W. G. Park, S. Cho, U. Kim, S.-J. Oh, B.-G. Park, F.- H. Chang, H.-J. Lin, and C. S. Hwang, *Phys. Status Solid RRL*, **6**, 181 (2012).
22. X. Luo, A. A. Demkov, D. Triyoso, P. Fejes, R Gregory, and S. Zollner, *Phys. Rev. B*, **78**, 245314 (2008).
23. G. Kresse and J. Hafner, *Phys. Rev. B*, **47**, 558(R) (1993); **49**, 14251 (1994).
24. P. E. Blochl, *Phys. Rev. B*, **50**, 17953 (1994).
25. J. P. Perdew, K. Burke, and M. Ernzerhof, *Phys. Rev. Lett.*, **77**, 3865 (1996).
26. G. Makov and M. C. Payne, *Phys. Rev. B*, **51**, 4014 (1995).
27. D.-Y. Cho, H.-S. Jung, and C. S. Hwang, *Phys. Rev. B*, **82**, 094104 (2010).
28. H. Miura, K. Suzuki, Y. Ito, S. Samukawa, T. Kubota, T. Ikoma, and H. Yoshikawa, in *Proc. Int. Reliab. Phys. Symp.* 2009, 376.